TECHNISCHE MECHANIK, 32, 2-5, (2012), 174 – 188
submitted: November 7, 2011

Diffuse Cohesive Energy in Plasticity and Fracture

G. Del Piero, G. Lancioni and R. March

In this paper we anticipate some results of a work in progress (Del Piero et al., 2012), in which the phenomena of fracture and yielding are described by a cohesive energy model, and fracture is regarded as a consequence of an extreme localization of the inelastic deformation. We first study a local model, which is successful in describing a number of aspects of the experimentally observed response, but fails to describe the phenomenon of strain softening. Indeed the model's prediction is that, just after its appearance, the inelastic deformation localizes, growing in an uncontrolled way and determining a catastrophic rupture. A more gradual growth is obtained by introducing a non-local energy term. Some numerical experiments show the great flexibility of the improved model: depending on the analytical shape assumed for the cohesive energy, the non-local model describes different types of response, such as yielding without fracture, ductile fracture with and without strain softening, and brittle fracture.

1 Introduction

The interest in variational models for fracture mechanics was originated by the paper (Francfort and Marigo, 1998), based on Griffith's theory of brittle fracture (Griffith, 1920). In this theory, fractures are represented as discontinuities of the displacement field along singular surfaces. The same representation is adopted in the cohesive energy models, introduced in (Barenblatt, 1962) and (Dugdale, 1960) to describe the ductile fracture modes which prevail in small-size bodies. In the cohesive energy models, fracture is preceded by a regime of large inelastic deformations, concentrated on the fracture surface. According to the analytic shape assumed for the cohesive energy, very different responses, such as plastic behavior, damage, brittle and ductile fracture, can be obtained, see (Del Piero and Truskinovsky, 2009).

There is a third fracture mode, in which the inelastic deformation initially spreads over a portion of the volume, called the *process zone*. Due to the progressive weakening of the material in this zone, the deformation eventually localizes on a fracture surface. A first description of this fracture mode was obtained by including in the energy balance the work done by the plastic deformation (Irwin, 1957). In recent variational approaches, the weakening of the material is attributed either to yielding (Dal Maso and Toader, 2010) or to damage (Babadjian, 2011), (Pham et al., 2010). In the present paper, which anticipates some results of a forthcoming paper (Del Piero et al., 2012), a description in terms of plasticity comes out, somehow unexpectedly, from the assumptions made on the shape of the energy. As discussed in the same paper, an appropriate modification of these assumptions leads to the damage model treated in (Pham et al., 2010).

We consider the one-dimensional case of a bar subject to given axial displacements u at the endpoints. For it we assume that, at every point x of the bar's axis, the axial deformation $u'(x)$ is the sum of an elastic part $\epsilon(x)$ and of an inelastic part $\gamma(x)$. We also assume that the energy of the bar is the sum of an elastic part and a cohesive part, with volume densities w and θ, respectively

$$\int_0^l \big(w(\epsilon(x)) + \theta(\gamma(x))\big)\, dx\,.$$

Finally, while the elastic part of the energy is totally reversible, the cohesive part is assumed to be dissipative.

With this simple model, we proceed by incremental energy minimization. With respect to the original *global minimization* of (Francfort and Marigo, 1998), there are two important changes. The first is that the minimization is now *local* instead of global, and the second is that it is *incremental*. Both improvements, already present in the concentrated cohesive energy model of (Del Piero and Truskinovsky, 2009), were made possible by the recent progress in the physical understanding and mathematical modelling of rate-independent evolutionary problems.

The essentials of incremental energy minimization and a comparison with other current solution methods can be found in the lecture notes (Mielke, 2011).

In the model for fracture described above, the result of incremental energy minimization is an accurate description of the bar's response, from the onset of inelastic deformation up to rupture. Some typical features of elastic-plastic response, such as yield condition, hardening rule, elastic unloading, are recovered as necessary conditions for an energy minimum.

The model is not completely satisfactory, since it fails to describe the *softening response* which precedes the ultimate rupture. Before rupture, the experiments show a more or less important regime in which the force-elongation response curve has a negative slope. This softening regime has the effect of increasing the ductility, with the consequence that the body can sustain a larger load without breaking.

The softening response is captured by adding to the energy a non-local term proportional to the square of the derivative of the inelastic deformation

$$\int_0^l \big(w(\epsilon(x)) + \theta(\gamma(x))\big)\, dx + \frac{1}{2}\,\alpha \int_0^l {\gamma'}^2(x)\, dx$$

with α a positive material constant. This procedure is known as the *singular perturbation* method. It is also called the *Van der Waals - Cahn Hilliard* method, due to the well known applications to the capillarity of fluids in (Van der Waals, 1873), and to phase transitions in (Cahn and Hilliard, 1958). More recent (Gurtin and Anand, 2005) is the application to crystal plasticity.

In both models, local and non-local, the localization of the inelastic strain occurs when the cohesive energy density θ is concave near the origin, that is, when $\theta''(0) < 0$. But, while in the local model the localization is immediately followed by rupture, in the non-local model a regime of inelastic deformation takes place. In this case, different types of response become possible. They are determined by the ratio between the length l of the bar and the material constant

$$l_i \,=\, \pi \sqrt{\frac{\alpha}{-\theta''(0)}}\ ,$$

which has the physical meaning of an *internal length* of the material. Indeed, for sufficiently low values of l/l_i the model predicts a totally ductile response, with the inelastic deformation growing all over the body and with no catastrophic failure. For higher values of l/l_i, the final rupture is preceded by a non-localized work-hardening regime and, for still higher values, by a localized softening regime. For fixed l_i and varying l, this reflects the well known *size effect* of fracture mechanics.

2 The Local Model

Consider a bar of length l, with constant cross section, free of external loads, and subject to the axial displacements

$$u(0) = 0\,, \qquad u(l) = \beta l \tag{1}$$

at the endpoints. The bar's deformation is measured by the derivative u' of the axial displacement u, and we assume that, at each point x of the bar's axis, $u'(x)$ can be decomposed into the sum of an elastic part $\epsilon(x)$ and an inelastic part $\gamma(x)$

$$u'(x) = \epsilon(x) + \gamma(x)\,. \tag{2}$$

The pair of functions (ϵ, γ) will be called a *configuration* of the bar. We assume that the strain energy of the bar is the sum of two terms, the elastic strain energy and the cohesive energy, with volume densities w and θ, respectively,

$$E(\epsilon, \gamma) = \int_0^l w(\epsilon(x))\, dx \,+\, \int_0^l \theta(\gamma(x))\, dx\,, \tag{3}$$

and that the axial force σ is related to the elastic deformation by the constitutive equation

$$\sigma(x) = w'(\epsilon(x))\,. \tag{4}$$

The function w is assumed to be strictly convex, and θ is assumed to be strictly increasing. Finally, we assume that w can be stored, while θ is totally dissipated. This requires that, in every deformation process $t \mapsto u(t)$, the cohesive power be non-negative at all x and for all t:

$$\theta'(\gamma(x,t))\,\dot\gamma(x,t) \geq 0\,.$$

For θ is strictly increasing, the *dissipation inequality*

$$\dot\gamma(x,t) \geq 0 \tag{5}$$

must be satisfied at all x and for all t.

2.1 Equilibrium

A perturbation of a configuration (ϵ,γ) is a pair $(\delta\epsilon,\delta\gamma)$ such that $\delta\epsilon(x) = \dot\epsilon(x)$ and $\delta\gamma(x) = \dot\gamma(x)$, for some deformation process $t \mapsto (\epsilon(t),\gamma(t))$ starting from (ϵ,γ). The dissipation inequality then implies $\delta\gamma(x) \geq 0$ at every point x of the bar.

In a variational approach, the equilibrium configurations are identified with the pairs (ϵ,γ) for which the first variation of the energy

$$\delta E(\epsilon,\gamma,\delta\epsilon,\delta\gamma) \;=\; \int_0^l \big(w'(\epsilon(x))\,\delta\epsilon(x) + \theta'(\gamma(x))\,\delta\gamma(x)\big)\,dx \tag{6}$$

is non-negative for arbitrary perturbations $\delta\epsilon$ and for all perturbations $\delta\gamma$ which preserve the length of the bar and satisfy the condition $\delta\gamma(x) \geq 0$ for all x. It is shown in (Del Piero et al., 2012) that an equilibrium configuration is characterized by the two following conditions:

(i) the axial force σ and the elastic deformation ϵ, which are related by the constitutive equation (4), are constant all over the bar,

(ii) the axial force is bounded from above by

$$\sigma \leq \theta'(\gamma(x)) \qquad \forall x \in (0,l)\,. \tag{7}$$

For an equilibrium configuration, the set of all points of the bar at which inequality (7) is strict

$$\mathcal{E} \;=\; \big\{\, x \in (0,l) \quad | \quad \sigma < \theta'(\gamma(x)) \,\big\}$$

is the *elastic zone*, and the complementary set $\mathcal{J} \;=\; (0,l) \setminus \mathcal{E}$, at which (7) holds as an equality, is the *inelastic zone*.

In the language of Plasticity, the equilibrium condition (7) is a *yield condition*, and $\theta'(\gamma(x))$ is a *yield limit*, depending on the punctual values of the inelastic deformation γ. Note that, in the present variational approach, this limit is not assumed a priori, but is obtained as a necessary condition for equilibrium.

Among all equilibrium configurations, of interest are those which are global or local energy minimizers. A necessary condition for an energy minimum is the non-negativeness of the second variation. It is proved in (Del Piero et al., 2012) that this occurs only if

$$\theta''(\gamma(x,t)) \geq 0 \tag{8}$$

almost everywhere in the inelastic zone $\mathcal{J}$. In the same paper it is proved that a slightly stronger condition is sufficient for a *strong local minimum*, that is, for a local minimum in the class of all perturbations $\delta\gamma$ such that

$$\sup_{x\in(0,l)} |\delta\gamma(x)| < \eta$$

for some fixed $\eta > 0$.

2.2 Quasi-Static Evolution

For a given loading process $\beta = \beta(t)$, assume that the equilibrium configuration $\epsilon(t), \gamma(x,t)$ at time t is known, and that we wish to determine the equilibrium configuration at time $t+\tau$. This can be done by incremental energy minimization. That is, by considering the expansion

$$E(\epsilon(t+\tau), \gamma(x,t+\tau)) \;=\; E(\epsilon(t), \gamma(x,t)) + \tau\, \dot{E}(\epsilon(t), \gamma(x,t)) + \frac{1}{2}\,\tau^2 \ddot{E}(\epsilon(t), \gamma(x,t)) + o(\tau^2)\,, \tag{9}$$

and minimizing for sufficiently small $\tau > 0$. On the right-hand side, the zero-order term is known. Then a first-order approximation is obtained by minimizing the functional $\dot{E}(\epsilon(t), \gamma(x,t))$. Note that, by (1) and (2),

$$\beta l = \int_0^l u'(x)\, dx = \int_0^l (\epsilon(x) + \gamma(x))\, dx\,,$$

so that, by the constancy of $\epsilon(x)$ in an equilibrium configuration,

$$\bar{\gamma} \doteq \frac{1}{l}\int_0^l \gamma(x)\, dx \;=\; \beta - \epsilon\,. \tag{10}$$

Then, by time differentiation of (3) and by the constitutive equation (4),

$$\dot{E}(\epsilon(t), \gamma(x,t)) \;=\; l\sigma(t)\,\dot{\beta}(t) + \int_0^l \big(\theta'(\gamma(x,t)) - \sigma(t)\big)\,\dot{\gamma}(x,t)\, dx\,. \tag{11}$$

On the right side everything is known except $\dot{\gamma}$, and the integrand function is non-negative by the equilibrium condition (7) and the dissipation inequality (5). Then the minimum of $\dot{E}(t)$ is achieved when the integrand function is zero. This fact, together with inequalities (5) and (7), determines the Kuhn-Tucker conditions

$$\dot{\gamma}(x,t) \geq 0\,, \quad \theta'(\gamma(x,t)) - \sigma(t) \geq 0\,, \quad \big(\theta'(\gamma(x,t)) - \sigma(t)\big)\,\dot{\gamma}(x,t) = 0\,, \tag{12}$$

for all x in $(0,l)$. The third condition, called the complementarity condition, states that $\dot{\gamma}(x,t)$ must be zero at all points of the elastic zone $\mathcal{E} = \mathcal{E}(t)$. It is remarkable that this assumption of classical Plasticity is obtained here as a necessary condition for incremental energy minimization.

No further information can be obtained from the first-order minimization. Indeed, if the complementarity condition holds then the integral term in (11) becomes equal to zero, and the minimum of $\dot{E}$ is equal to $l\sigma(t)\dot{\beta}(t)$. To determine $\dot{\gamma}(x,t)$ in the inelastic zone, it is necessary to consider the second-order approximation of the functional (9). This leads to the minimization of the second-order term $\ddot{E}(\epsilon(t), \gamma(x,t))$ in the expansion of the energy. It is shown in (Del Piero et al., 2012) that this minimization determines a second set of Kuhn-Tucker conditions

$$\dot{\gamma}(x,t) \geq 0\,, \quad \theta''(\gamma(x,t))\,\dot{\gamma}(x,t) - \dot{\sigma}(t) \geq 0\,, \quad \big(\theta''(\gamma(x,t))\,\dot{\gamma}(x,t) - \dot{\sigma}(t)\big)\,\dot{\gamma}(x,t) = 0 \tag{13}$$

for all x in $\mathcal{J}(t)$. The first condition is again the dissipation inequality. The second is a relation between the increments of the force and of the inelastic deformation in the inelastic zone. In it, equality denotes the permanence of x in the inelastic zone, and strict inequality denotes the return of x inside the elastic zone. The third is the *consistency condition*, which says that $\dot{\gamma}(x)$ must be zero when x returns inside the elastic zone. Again, some assumptions of classical Plasticity are obtained here as necessary conditions for second-order incremental minimization.

2.3 Evolution from the Natural Configuration

Consider a loading process $t \mapsto \beta(t)$ with $\dot{\beta}(t) > 0$ for all $t \geq 0$, starting from the natural configuration $(\epsilon(0)\,, \gamma(x,0)) = (0,0)$, at $t = 0$. For this process, there is a time interval $(0, t_c)$ at which the evolution is purely elastic, that is,

$$\gamma(x,t) = 0 \quad \forall x \in (0,l)\,, \qquad \epsilon(t) = \beta(t)\,, \qquad \sigma(t) = w'(\beta(t))\,. \tag{14}$$

This elastic regime ends at the time t_c at which β reaches the critical value

$$\beta_c = \beta(t_c) = (w')^{-1}(\theta'(0))\,. \tag{15}$$

At time t_c, inequality (7) is satisfied as an equality. Then all points of the bar switch from the elastic to the inelastic zone, and a regime of inelastic deformation begins. The subsequent evolution strongly depends on the sign of $\theta''(0)$.

If $\theta''(0) > 0$, because $\dot\gamma(x,t)$ has to be positive for some x, from the complementarity condition $(13)_3$ it follows that $\dot\sigma(t)$ is positive. Then, by inequality $(13)_2$, $\dot\gamma(x,t_c)$ has the constant value

$$\dot\gamma(x,t_c) \,=\, \frac{\dot\sigma(t_c)}{\theta''(0)} \;. \tag{16}$$

Then $\gamma(x,t)$ is constant at the instants immediately following t_c. This conclusion holds for all $t > t_c$, as long as $\theta''(\gamma(t))$ keeps a positive value. Therefore, we have the homogeneous evolution

$$\dot\gamma(x,t) \,=\, \frac{\dot\sigma(t)}{\theta''(\gamma(t))} \,=\, \bar{\dot\gamma}(t)\,.$$

Together with the relations

$$\dot\epsilon(t) \,=\, \dot\beta(t) - \bar{\dot\gamma}(t)\,, \qquad \dot\sigma(t) = w''(\epsilon(t))\,(\dot\beta(t) - \bar{\dot\gamma}(t))\,, \tag{17}$$

which follow from (10) and (4), respectively, this relation determines the incremental force-elongation response

$$\dot\sigma(t) = \frac{\theta''(\gamma(t))\,w''(\epsilon(t))}{\theta''(\gamma(t)) + \,w''(\epsilon(t))}\;\dot\beta(t)\,. \tag{18}$$

As long as $\theta''(\gamma(t))$ remains positive, the slope $\dot\sigma/\dot\beta$ of the response curve (σ,β) is positive. That is, the response is *work-hardening*.

This conclusion holds only for processes with $\dot\beta(t) > 0$ for all t. Indeed, from $(17)_2$ and from the complementarity condition $(13)_3$ it follows that

$$w''(\epsilon(t))\,\dot\beta(t)\,\dot\gamma(x,t) \,=\, (\theta''(\gamma(t)) + w''(\epsilon(t)))\,\bar{\dot\gamma}(t)\,\dot\gamma(x,t)\,. \tag{19}$$

Because the parenthesis on the right-hand side is positive, for $\dot\beta \le 0$ it must be $\dot\gamma(x,t) = 0$ at all x, that is, elastic unloading takes place.

If $\theta''(0) = 0$, or if, during the hardening response, $\theta''(\gamma(t))$ becomes zero at some t, from equation (19) we still have elastic unloading for $\dot\beta(t) \le 0$. For $\dot\beta(t) > 0$ the same equation yields $\bar{\dot\gamma}(t) = \dot\beta(t)$, while the punctual distribution of $\dot\gamma$ remains undetermined. Note that, by $(17)_2$, $\bar{\dot\gamma}(t) = \dot\beta(t)$ implies $\dot\sigma(t) = 0$, that is, a *perfectly plastic* response.

Finally, if $\theta''(\gamma(x,t))$ is negative at some (x,t), the necessary condition (8) for an energy minimum is violated. In this case it is easy to see that, if $\theta''(\gamma(\,\cdot\,,t))$ is negative on a set of finite measure, the term $\ddot E$ in the expansion (9) of the energy attains arbitrarily large negative values when $\dot\gamma$ concentrates over smaller and smaller portions of that set. The dropping of the energy to $-\infty$ is the model's representation of the catastrophic failure of the bar.

3 The Non-Local Model

The indeterminacy of the spatial distribution of the inelastic strain rate and the absence of a strain softening response are two major defects of the model discussed so far. They can be eliminated by adding to the energy (3) a non-local term proportional to the square of the derivative of the inelastic deformation

$$E_\alpha(\epsilon,\gamma) = \int_0^l \big(w(\epsilon(x)) + \theta(\gamma(x)) + \tfrac{1}{2}\,\alpha{\gamma'}^2(x)\big)\,dx\,, \tag{20}$$

where α is a small positive constant.

The addition of the non-local term requires some regularity of γ. Here we assume that γ is $C^1[0,l]$. An extension to functions with a discontinuous first derivative does not change substantially the results, see (Del Piero et al., 2012).

3.1 Equilibrium

Like in the local model, an equilibrium confiuration (ϵ, γ) is characterized by the non-negativeness of the first variation of the energy

$$\delta E_\alpha(\epsilon, \gamma, \delta\epsilon, \delta\gamma) = \int_0^l \big(w'(\epsilon(x))\,\delta\epsilon(x) + \theta'(\gamma(x))\,\delta\gamma(x) + \alpha\gamma'(x)\,\delta\gamma'(x)\big)\,dx$$

for all perturbations $(\delta\epsilon, \delta\gamma)$ which satisfy the dissipativity condition $\delta\gamma(x) \geq 0$ at all x, and which preserve the length of the bar. This condition again requires that in an equilibrium configuration the axial force σ and the elastic deformation ϵ be constant over the bar, and that the inequality

$$\sigma \leq \theta'(\gamma(x)) - \alpha\gamma''(x) \tag{21}$$

be satisfied at all x (Del Piero et al., 2012). This is the non-local counterpart of the yield condition (7). With it, the elastic and inelastic zone are re-defined by

$$\mathcal{E}_\alpha \,=\, \big\{\, x \in (0,l) \quad | \quad \sigma < \theta'(\gamma(x)) - \alpha\gamma''(x) \,\big\}\,, \qquad \mathcal{J}_\alpha \,=\, (0,l) \setminus \mathcal{E}_\alpha\,,$$

respectively. The analysis of the first variation also provides some additional boundary conditions. It is possible, see (Del Piero et al (Del Piero et al., 2012)), to choose between two possible alternatives

$$\gamma'(l) \,=\gamma'(0) = 0\,, \qquad \text{and} \qquad \gamma(l) \,=\gamma(0) = 0\,. \tag{22}$$

The first alternative produces solutions in which the inelastic deformation concentrates at the ends of the bar, while with the second alternative the inelastic deformation concentrates at the interior. The second choice is preferable, because it allows a closer comparison with the experimental results. Indeed, in the experiments the concentration of the inelastic deformation at the ends is avoided, either by reinforcing the terminal parts of the bar, or by weakening the central part with the creation of a notch. As a consequence of our choice of the boundary conditions $(22)_2$, the requirements on the admissible perturbations $\delta\gamma$ in the analysis of the variations of E_α must be completed by the conditions

$$\delta\gamma(l) = \delta\gamma(0) = 0\,. \tag{23}$$

The gradient term introduced in the non-local model has a stabilizing effect, because it adds a positive term to the second variation of the energy. It is proved in (Del Piero et al., 2012) that this term renders the second variation non-negative when the zero on right-hand side of inequality (8) is replaced by a negative constant, depending on l and on the Young modulus of the material.

In the same paper (Del Piero et al., 2012), some sufficient conditions for a local minimum are proved. Here they will be considered later, and only for equilibrium configurations at the onset of the inelastic regime. They allow for the presence of negative values of $\theta''(\gamma(x))$, not allowed in the local model because of the necessary condition (8). This makes possible a description of strain softening within the non-local model.

3.2 Quasi-Static Evolution

In order to determine the evolution of the bar in a loading process $t \mapsto \beta(t)$, we consider the expansion (9) for the energy E_α. The first-order term in the expansion is

$$\begin{aligned}
\dot{E}_\alpha(t) \;&=\; \int_0^l \big(w'(\epsilon(t))\,\dot\epsilon(t) + \theta'(\gamma(x,t))\,\dot\gamma(x,t) + \alpha\gamma'(x,t)\,\dot\gamma'(x,t)\big)\,dx \\
&=\; l\dot\beta(t)\,\sigma(t) + \int_0^l \big(\theta'(\gamma(x,t)) - \sigma(t) - \alpha\gamma''(x,t)\big)\,\dot\gamma(x,t)\,dx + \alpha\Big[\gamma'(x,t)\,\dot\gamma(x,t)\Big]_0^l\,.
\end{aligned}$$

On the right-hand side, the integrand function is non-negative by the dissipation inequality (5) and the equilibrium condition (21), and the boundary term is zero by the boundary conditions

$$\dot\gamma(l,t) = \dot\gamma(0,t) = 0\,, \tag{24}$$

which follow from (23). Therefore, the minimum of $\dot{E}_\alpha(t)$ is $l\dot{\beta}(t)\,\sigma(t)$, and the minimizers satisfy the Kuhn-Tucker conditions

$$\begin{aligned} &\dot\gamma(x,t)\,\geq\,0\,,\quad \theta'(\gamma(x,t))-\sigma(t)-\alpha\gamma''(x,t)\,\geq\,0\\ &\quad\big(\theta'(\gamma(x,t))-\sigma(t)-\alpha\gamma''(x,t)\big)\,\dot\gamma(x,t)\,=\,0 \end{aligned} \tag{25}$$

for all x in $(0,l)$, and the boundary conditions (24). Just as in the local model, the complementarity condition $(25)_3$ states that $\dot\gamma(x,t)=0$ at all points in the elastic zone $\mathcal{E}_\alpha(t)$. As shown in (Del Piero et al., 2012), the minimization of the second-order term $\ddot{E}_\alpha$ in the expansion of E_α determines a second set of Kuhn-Tucker conditions

$$\begin{aligned} &\dot\gamma(x,t)\geq 0\,,\quad \theta''(\gamma(x,t))\,\dot\gamma(x,t)-\dot\sigma(t)-\alpha\,\dot\gamma''(x,t)\geq 0\\ &\quad\big(\theta''(\gamma(x,t))\,\dot\gamma(x,t)-\dot\sigma(t)-\alpha\,\dot\gamma''(x,t)\big)\,\dot\gamma(x,t)=0 \end{aligned} \tag{26}$$

to be satisfied by all x in $\mathcal{J}_\alpha(t)$. These are non-local versions of conditions (13).

Added in proof. Futher investigation, made after this paper was written, showed that conditions (26) hold only approximately. There is indeed a supplementary term, inherited from the first-order minimization, which does not disappear in the limit when the time step in the expansion (9) tends to zero, see (Del Piero et al., 2012) for details. Ignoring this term gave some trouble in reproducing the response curve of concrete, which, for this reason, was excluded from the present communication. The supplementary term does not affect the analysis of the response at the onset of the inelastic regime, made in the following Section. In the numerical scheme of Section 4, the functional (42) should be completed with the addition of an extra term. This change does not affect the numerical results on the steel bar presented in Section 5.

3.3 The Onset of the Inelastic Regime

Like in the local model, in a loading process $t\mapsto\beta(t)$ with $\dot\beta(t)>0$ starting from the natural configuration there is an initial time interval $(0,t_c)$ in which the evolution is purely elastic. That is, the deformation is homogeneous, and $\gamma(x,t)$, $\epsilon(t)$ and $\sigma(t)$ are as in (14). When t reaches the time t_c given by (15), all points in the bar switch from the elastic to the inelastic zone, and an inelastic regime takes place.

By the complementarity condition $(26)_3$, the equation (16) of the local model is now replaced by the differential equation

$$\theta''(0)\,\dot\gamma(x)-\dot\sigma-\alpha\,\dot\gamma''(x)=0\,, \tag{27}$$

where the dependence on the constant $t=t_c$ has been omitted. This equation is associated with the boundary conditions (24). Therefore, just as in the local model, the evolution in the inelastic regime depends on the sign of $\theta''(0)$. If $\theta''(0)>0$, the solution is

$$\dot\gamma(x)=\frac{\dot\sigma}{\theta''(0)}\left(\tanh\frac{\kappa l}{2}-\tanh\frac{\kappa x}{2}\right)\,\sinh\kappa x\,, \tag{28}$$

where $\kappa=(\theta''(0)/\alpha)^{1/2}$. Computing the average $\bar{\dot\gamma}$ and using the constitutive equation (4), the incremental force-elongation response

$$\dot\sigma\;=\;\frac{w''(\beta_c)\;\theta''(0)}{\theta''(0)+\varphi(\kappa l)\,w''(\beta_c)}\;\dot\beta\,,\qquad \varphi(\kappa l)\;\doteq\;1-\;\frac{\tanh\kappa l/2}{\kappa l/2}\;, \tag{29}$$

follows. A comparison with the local counterpart (18) shows that the non-local effect is given by the factor $\varphi(\kappa l)$, which is positive and less than one.

For $\theta''(0)=0$, the solution is

$$\dot\gamma(x)=\frac{\dot\sigma}{2\alpha}\;x\,(l-x)\,,\qquad \dot\sigma\;=\;\frac{12\alpha\,w''(\beta_c)}{12\alpha+l^2w''(\beta_c)}\;\dot\beta\,. \tag{30}$$

Thus, for $\theta''(0)\;\geq\;0$ the non-local energy term has the effect of increasing the slope of the force-elongation response curve. In particular, for $\theta''(0)=0$ a hardening response takes the place of the perfectly plastic response

$\dot\sigma = 0$ predicted by the local model, and the indeterminacy of the punctual values $\dot\gamma(x)$ exhibited by the local model now disappears.

For $\theta''(0) < 0$, there are two types of solutions: *full-size solutions*, in which $\dot\gamma(x)$ is positive all over the bar, and *localized solutions*, in which $\dot\gamma(x)$ is positive on a proper subset of $(0, l)$. The full-size solution is

$$\dot\gamma(x) = \frac{\dot\sigma}{\theta''(0)} \left(\tan\frac{kx}{2} - \tan\frac{kl}{2} \right) \sin kx \,, \tag{31}$$

where $k = (-\theta''(0)/\alpha)^{1/2}$. For the singular case $kl = \pi$, for which $\tan kl/2$ is infinite, the solution is

$$\dot\gamma(x) = \frac{\pi}{2}\, \dot\beta \, \sin\frac{\pi x}{l} \,. \tag{32}$$

To be admissible, a solution must satisfy the dissipation inequality $\dot\gamma(x) \geq 0$ at all x. It is easy to verify that this is true for the solutions (28), (30) for $\theta''(0) \geq 0$. For $\theta''(0) < 0$, the solutions (31), (32) satisfy the dissipation inequality for $0 < kl \leq \pi$, while for all $kl > 2\pi$ the same condition is violated. In the remaining interval $\pi < kl \leq 2\pi$, the dissipation inequality is satisfied only if

$$\theta''(0) + \psi(kl)\, w''(\beta_c) > 0 \,, \qquad \psi(kl) \doteq 1 - \frac{\tan kl/2}{kl/2} \,. \tag{33}$$

Let kl_c be the value of kl for which the above inequality is satisfied as an equality. Because the function ψ is decreasing in the interval $(\pi, 2\pi)$, inequality (33) is the same as

$$kl \,<\, kl_c \,. \tag{34}$$

Then, the full-size solution (31) is admissible for $kl \leq \max\{\, 2\pi, kl_c\}$. The corresponding incremental force-elongation relation is

$$\dot\sigma = \frac{\theta''(0)\, w''(\beta_c)}{\theta''(0) + \psi(kl)\, w''(\beta_c)}\, \dot\beta \;, \tag{35}$$

with $\dot\sigma = 0$ in the singular case $kl = \pi$. The study of the function ψ shows that $\psi(kl)$ is negative for $kl < \pi$ and positive for $\pi < kl < 2\pi$. Then the slope $\dot\sigma/\dot\beta$ of the response curve (σ, β) is positive for $kl < \pi$, zero for $kl = \pi$, and negative for $\pi < kl < \max\{\, 2\pi, kl_c\}$. In the three cases, the response at the onset of the inelastic deformation is work-hardening, perfectly plastic, and strain-softening, respectively. If $kl_c < 2\pi$, for $kl = kl_c$ the denominator in (35) is zero, that is, the negative slope of the response curve becomes infinite. In the present non-local model, this situation is identified with the final rupture of the bar. Then, if $kl \geq kl_c$, rupture takes place immediately after the onset of the inelastic deformation. This is the model's representation of Griffith's brittle fracture.

Now consider a localized solution with $\dot\gamma(x)$ positive on an interval $(a, a+l_y)$ strictly contained in $(0, l)$ and zero outside. In it, $\dot\gamma$ satisfies the differential equation (27) at the interior points of the interval, and the conditions $\dot\gamma(a) = \dot\gamma(a+l_y) = 0$ at the boundary. These conditions come either from the boundary conditions (24) or from continuity with the neighboring region, at which $\dot\gamma(x) = 0$. Moreover, the assumed continuity of $\dot\gamma'(x)$ requires that $\dot\gamma'(a) = 0$ if $a > 0$ and $\dot\gamma'(a + l_y) = 0$ if $a + l_y < l$. In all cases, see (Del Piero et al., 2012), this results in the supplementary condition

$$l_y = \frac{2\,\pi}{k} \;, \tag{36}$$

which determines the extent l_y of the localization. The solution of the differential problem is

$$\dot\gamma(x) = \frac{\dot\sigma}{\theta''(0)} \big(1 - \cos k\,(x - a)\big) \,, \qquad x \in (a, a+l_y) \,. \tag{37}$$

By (36) with $l_y < l$, this solution is possible only if $kl > 2\pi$. That is, only for values of kl for which a full-size solution is not admissible. Moreover, the dissipation inequality is satisfied only if

$$\theta''(0) + \frac{2\pi}{kl}\, w''(\beta_c) > 0 \,. \tag{38}$$

Denote by kl_r the value of kl for which this inequality holds as an equality. By comparison with $(33)_1$ it follows that

$$\psi(kl_c) \,=\, \frac{2\pi}{kl_r}\,.$$

Because ψ is a decreasing function of kl, for $kl_c > 2\pi$ one has $\psi(kl_c) < \psi(2\pi) = 1$ and, therefore, $kl_r > 2\pi$. Thus, if $kl_c > 2\pi$, that is, if the full-size solution (31) is admissible for all $kl \le 2\pi$, then there is an interval $(2\pi, kl_r)$ in which the localized solution (37) is admissible. On the contrary, no localized solution is admissible if $kl_c < 2\pi$. For $2\pi < kl < kl_c$, the incremental force-elongation relation is

$$\dot\sigma \,=\, \frac{\theta''(0)\, w''(\beta_c)}{\theta''(0) + \frac{2\pi}{kl}\, w''(\beta_c)}\,\dot\beta\,. \tag{39}$$

By (38), the slope of the (σ, β) response curve is negative. That is, at the onset of the inelatic deformation a localized solution corresponds to a strain-softening response. Brittle fracture, again characterized by an infinite negative slope of the response curve, occurs for all kl greater than kl_r.

The results of preceding analysis are better expressed in terms of the internal length

$$l_i \,=\, \pi\sqrt{\frac{\alpha}{-\theta''(0)}}\,. \tag{40}$$

Indeed, at the onset of the inelastic regime we have

(i) a full-size solution with a work-hardening response if $l \le l_i$,

(ii) a full-size solution with a strain-softening response if $l_i < l \le \max\{\, 2l_i, l_c\}$,

(iii) a localized solution with a strain-softening response if $2l_i < l < l_r$,

(iv) brittle fracture if $\, l \le l_c < 2\pi/\, k \,$ and if $\, l > l_r > 2\pi/\, k$.

Beyond the onset of the inelastic deformation, the differential equation (27) is replaced by

$$\theta''(\gamma(x))\,\dot\gamma(x) - \alpha\dot\gamma''(x) \,=\, \dot\sigma \tag{41}$$

with $\gamma(x)$ not anymore constant. This equation cannot be solved, in general, in a closed form. Then, the quasi-static evolution can be determined only approximately, using step-by step numerical algorithms. Like at the onset, a solution may be full-size or localized, or brittle fracture may occur, depending on material parameters more difficult to evaluate. Some general properties of the evolution are proved in (Del Piero et al., 2012):

- The continuation is full-size if $\theta''(\gamma(x)) > 0$ at all x in the inelastic region $\mathcal{J}_\alpha$,
- $\dot\sigma$ is negative if $\theta''(\gamma(x)) \le 0$ at all x in $\mathcal{J}_\alpha$,
- in a localized continuation the process zone of the inelastic deformation tends to concentrate over smaller and smaller regions if the derivative θ' is concave, and to spread out over larger regions if θ' is convex.

4 The Numerical Scheme

For a given load process $t \mapsto \beta(t)$, suppose that the equilibrium configuration $(\varepsilon(t), \gamma(x,t))$ at time t is known. Then the configuration at the time $t + \tau$ is determined by minimizing the expansion (9) of the energy $E_\alpha(\epsilon, \gamma)$ at $(\epsilon(t), \gamma(x,t))$. As explained in Sections 2.2 and 3.2, the zero-order and the first-order term of the expansion are determined. Then a second-order approximation is obtained by minimizing the second-order term

$$\ddot E_\alpha(\beta(t), \gamma(x,t); \dot\gamma) \,=\, l w''(\beta(t) - \bar\gamma(t))(\dot\beta(t) - \bar{\dot\gamma})^2 + \int_{\mathcal{J}_\alpha(t)} \big(\theta''(\gamma(x,t))\,\dot\gamma^2(x) + \alpha\,\dot\gamma'^2(x)\big)\,dx\,, \tag{42}$$

in the class of all functions $\dot\gamma$ which satisfy the dissipation inequality (5) and the boundary conditions (24), and vanish in the elastic zone $\mathcal{E}_\alpha(t)$. The minimizer $\dot\gamma(x)$ provides the approximation

$$\gamma_\tau(x) \,=\, \gamma(x,t) + \tau\dot\gamma(x)\,,$$

for the deformation $\gamma(x, t+\tau)$. This approximation is refined by minimizing the quadratic approximation of E_α at γ_τ

$$E_{\alpha 2}(\beta(t+\tau), \gamma_\tau + \delta\gamma) \;=\; E_\alpha(\gamma_\tau) + \frac{\partial}{\partial\gamma} E_\alpha(\gamma_\tau)\,\delta\gamma + \frac{1}{2}\frac{\partial^2}{\partial\gamma^2} E_\alpha(\gamma_\tau)\,\delta\gamma^2, \tag{43}$$

where

$$\frac{\partial}{\partial\gamma} E_\alpha(\gamma_\tau)\,\delta\gamma \;=\; \int_{\mathcal{J}_\alpha(\gamma_\tau)} \big(\theta'(\gamma_\tau(x))\,\delta\gamma(x) + \alpha\gamma'_\tau(x)\,\delta\gamma'(x) - w'(\epsilon_\tau)\,\delta\gamma(x)\big)\,dx\,,$$
$$\frac{\partial^2}{\partial\gamma^2} E_\alpha(\gamma_\tau)\,\delta\gamma^2 = \int_{\mathcal{J}_\alpha(\gamma_\tau)} \big(\theta''(\gamma_\tau(x))\,\delta\gamma^2(x) + \alpha\,\delta\gamma'^{\,2}(x) + w''(\epsilon_\tau)\,\delta\gamma^2(x)\big)\,dx\,,$$

and

$$\epsilon_\tau = \beta(t+\tau) - \bar\gamma_\tau\,,$$
$$\mathcal{J}_\alpha(\gamma_\tau) \;=\; \big\{\, x \in (0,l) \quad | \quad w'(\epsilon_\tau) \;=\; \theta'(\gamma_\tau(x)) \,\big\}\,.$$

The algorithm to determine $\delta\gamma$ is the following.

0. *Initialization.* Set $\beta_0 = \beta(t)$, $\gamma_0(x) = \gamma(x,t)$.

1. *Incremental step.*

- (i) Compute $\dot\gamma_0 = \operatorname{argmin}\big\{\ddot E_\alpha(\beta_0, \gamma_0;\, \dot\gamma\,) \quad | \quad \dot\gamma(x) \ge 0,\ \dot\gamma(0) = \dot\gamma(l) = 0\big\}$.
- (ii) Set $\beta_1 = \beta(t+\tau)$, $\gamma_1^0(x) = \gamma_0(x) + \tau\dot\gamma_0(x)$.

2. *Iterative refinement, i-th step.*

- (i) Compute $\delta\gamma^i \;=\; \operatorname{argmin}\big\{\, E_{\alpha 2}(\beta_1, \gamma_1^{i-1}, \delta\gamma) \quad | \quad \delta\gamma(x) \;\ge\; \gamma_0(x) - \gamma_1^{i-1}(x), \quad \delta\gamma(0) \;=\; \delta\gamma(l) \;=\; 0\,\big\}$, and set $\gamma_1^i = \gamma_1^{i-1} + \delta\gamma^i$.
- (ii) Stop when the L^2 norm of $(\gamma_1^i - \gamma_1^{i-1})$ is less than a given tolerance $\hat\gamma$.

3. *End*

- (i) Take as γ_1 the last γ_1^i in step 2.
- (ii) If the L^2 norm of $(\gamma_1 - \gamma_0)$ is less than a given tolerance $\tilde\gamma$, perform a new incremental step starting from (β_1, γ_1). Otherwise, repeat the computation with τ replaced by $\tau/2$.

The last control avoids the overcoming of energy barriers due to excessively large incremental steps.

In the numerical code, the bar is discretized using linear finite elements. The quadratic programming problems involving the minimization of $\ddot E_\alpha$ and $E_{\alpha 2}$ are solved using the projection method (Gill et al., 1981,P) implemented in the *quadprog.m* function of Matlab. The code generates a mesh refinement when the number of elements in the inelastic region $\mathcal{J}_\alpha$ is smaller than a certain number, 100 in the simulations presented below. In this case, each element is split into two sub-elements.

In all simulations, for the elastic strain energy density we assume the quadratic expression

$$w(\epsilon) = \tfrac{1}{2}\,EA\,\epsilon^2$$

where the axial stiffness EA is the product of the Young modulus E of the material by the area A of the cross section, and for the cohesive energy density we take the piecewise cubic function

$$\theta(\gamma) = A_i + B_i\gamma + \tfrac{1}{2}\,C_i\gamma^2 + \tfrac{1}{6}\,D_i\gamma^3\,, \qquad \gamma \in [\gamma_{i-1}, \gamma_i\,]\,, \qquad i \in \{1 \ldots n\}\,, \tag{44}$$

where γ_i are a finite number of nodal points, with $\gamma_0 = 0$ and $\gamma_n \leq +\infty$. To guarantee the continuity of θ and of the derivatives θ', θ'' at the nodal points, the coefficients A_i, B_i, C_i, D_i must satisfy the $3n-3$ conditions

$$B_{i+1} = B_i - 3\,(A_{i+1}-A_i)(\gamma_{i+1})^{-1},\; C_{i+1} = C_i + 6\,(A_{i+1}-A_i)(\gamma_{i+1})^{-2},\; D_{i+1} = D_i - 6\,(A_{i+1}-A_i)(\gamma_{i+1})^{-3},$$

Then only $n+3$ of the $4n$ constants are independent. We take $A_1 = \theta(0) = 0$, while $B_1 = \theta'(0)$, the value of the force at the onset of the inelastic regime, is identified on the experimental curve. Then we are free to choose $n+1$ of the remaining constants. These constants can be used to identify a specific experimental response curve. In the next section, they are selected with the purpose of reproducing the experimental tensile test on a steel bar.

5 Numerical Simulations

A tension test was performed at the Laboratorio Prove Materiali e Strutture of the Università Politecnica delle Marche in Ancona, on a ribbed bar of B450C (FeB44k) steel, with diameter $\phi = 16$ mm, and with

$$l = 200\,\text{mm}\,, \quad EA = 42 \times 10^3\,\text{kN}\,, \quad B_1 = 109.5\,\text{kN}\,.$$

For the cohesive energy a convex-concave expression of the type (44) was taken, with

$$n = 3\,, \qquad \gamma_i = (0.10,\, 0.54,\, +\infty)\,,$$
$$C_1 = 400\,\text{kN}\,, \quad D_1 = -4000\,\text{kN}\,, \quad A_i = (0,\, -0.65,\, 28.03)\,\text{kN}\,.$$

The function $\theta(\gamma)$ is plotted in Fig. 1. It is convex for $\gamma < 0.1$, and concave for $\gamma > 0.1$.

We take $\beta = t$, so that the time-like parameter t is physically non-dimensional. For the non-locality parameter α, the time step τ, the initial mesh size h, and the tolerances $\hat{\gamma}$ and $\tilde{\gamma}$ we take

$$\alpha = 100\,\text{kN mm}^2, \quad \tau = 10^{-4}, \quad h = 1\,\text{mm}\,, \quad \hat{\gamma} = 10^{-6}\,, \quad \tilde{\gamma} = 10^{-3}\,.$$

In Fig. 2, the experimental response is represented by the dotted curve. It reaches the elastic limit at $\beta = 0.0026$, a maximum at $\beta = 0.1016$, and the slope becomes infinite at $\beta = 0.1254$. In the same figure, the solid line is the numerical response curve. The two curves are very close to each other. In particular, the numerical curve reproduces the hardening regime, $0.0026 < \beta < 0.1016$, and the softening regime, $0.1016 < \beta < 0.1254$, of the post-elastic evolution. In the simulation, the two regimes are determined by the convex and concave part of θ, respectively. With the addition of an initial concave part, the horizontal plateau shown by the experiment in the range ($0.0026 < \beta < 0.017$) could also be reproduced.

The evolution of the inelastic deformation is described in Fig. 3, where γ and $\dot{\gamma}$ are plotted for different values of β. In the hardening regime the inelastic deformation γ is almost constant over the bar, except near the boundary, where γ is zero by the boundary conditions (16). In the softening regime, in the short interval $0.1016 < \beta < 0.1018$ the evolution is still full-size as in the previous hardening regime. For $\beta > 0.1018$, the inelastic deformation gradually localizes on shorter and shorter intervals. The extreme localization is reached for $\beta = 0.1254$. At this point the response curve becomes vertical, and rupture occurs.

The diagrams of the localized inelastic deformation for different values of β are collected in Fig. 4a. They are in a very good qualitative agreement with the experimental curves of Fig. 4b, taken from (Miklowitz, 1950). In Fig. 5a the transverse profile of the bar is shown for β close to the rupture value 0.1254. This profile has been deduced from the axial deformation obtained in the simulation, assuming a coefficient of transverse contraction (Poisson's ratio) equal to 0.3. It is very similar to the profile in the picture of Fig. 5b, also taken from (Miklowitz, 1950).

To investigate the influence of the size l of the specimen and of the non-locality parameter α, we performed the following series of simulations:

Simulation	1	2	3	4	5	6	7	8	
l =	200	300	200	100	100	200	100	100	mm,
α =	100	100	50	25	100	500	300	500	kN mm^2.

Simulation 1 is the one used for comparison with the experiment. The response curves of Simulations 1, 2 and 5, all corresponding to the same α, are shown in Fig. 6. The three curves differ only in the softening part, which is shorter for larger l. That is, larger bars are less ductile, and break at for smaller values of β. This is a clear manifestation of the size effect.

The same loss of ductility and reduction of the rupture value β_r of β is observed when α is reduced keeping l constant. In Fig. 7, the values of β_r obtained in the eight simulations are plotted versus the ratio $\sqrt{\alpha}/l$. They almost exactly lie on a straight line. That is, for the rupture value of β our simulations provide the empirical relation

$$\beta_r \;=\; c_1 + c_2 \frac{\sqrt{\alpha}}{l}\,,$$

with c_1, c_2 suitable constants. Recalling the expression (40) of the internal length l_i, we can put this relation into the form

$$\beta_r \;=\; c_1 + c_2 \;\frac{\sqrt{-\theta''(0)}}{\pi}\;\;\frac{l_i}{l}\;\;,$$

which shows that the rupture load is governed by the ratio $l_i/\,l$. That is, the parameter l_i, which comes from the analysis of the onset of the inelastic deformation, seems to be useful to predict the elongation at rupture, at least when rupture occurs at the end of a substantial inelastic regime.

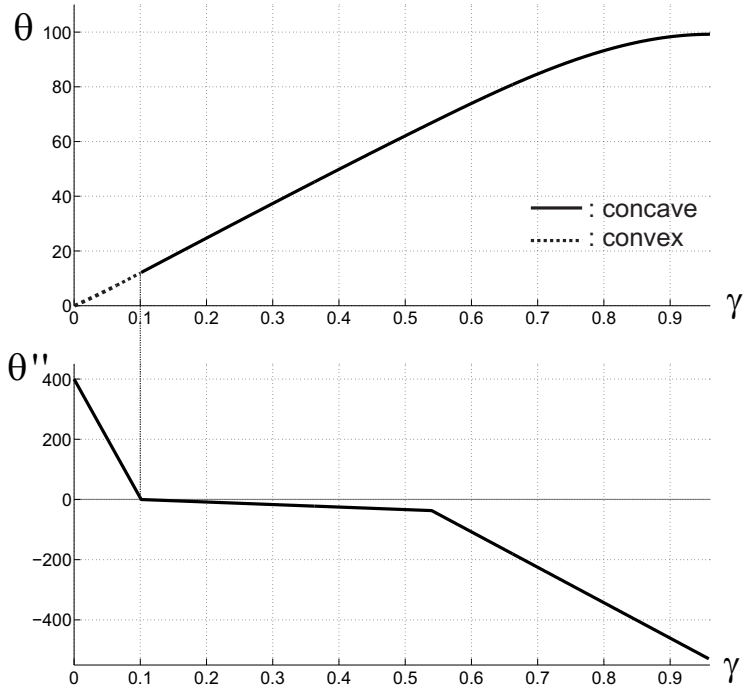

Figure 1. Graphs of $\theta(\gamma)$ (a), and of $\theta''(\gamma)$ (b)

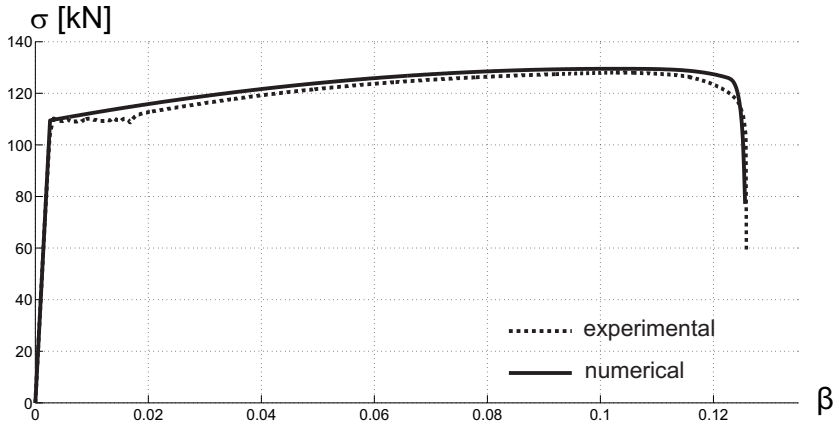

Figure 2. Force-elongation response curves: experimental (dotted line) and numerical (solid line)

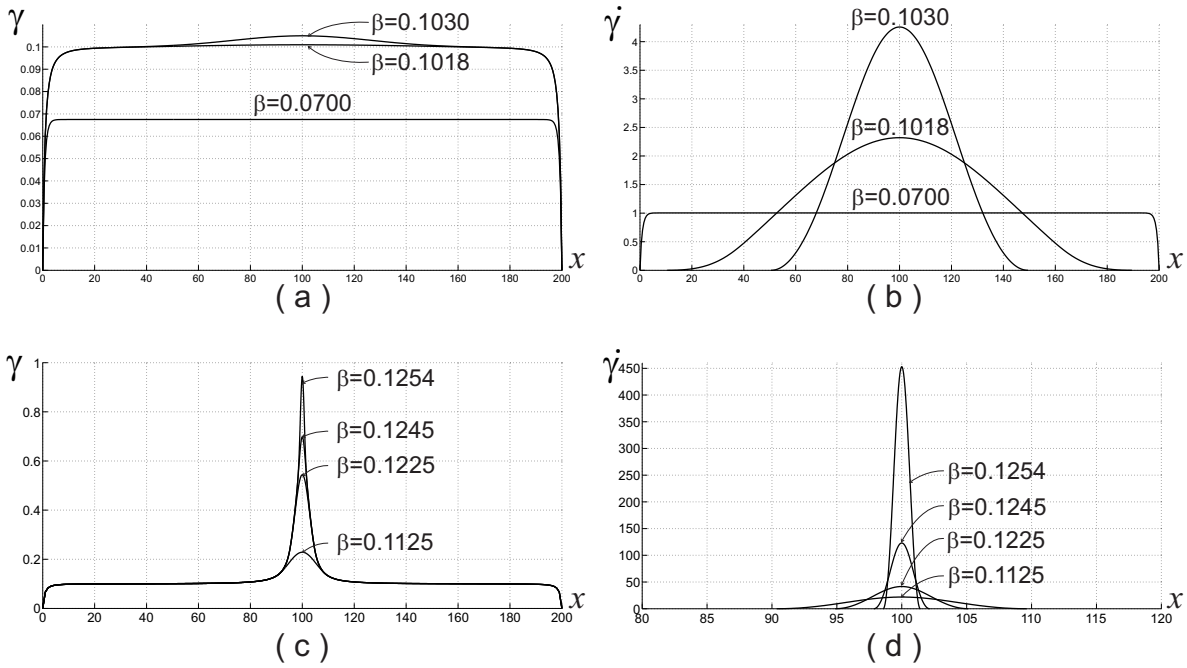

Figure 3. Diagrams of γ (a), (c) and $\dot{\gamma}$ (b), (d) for different values of β

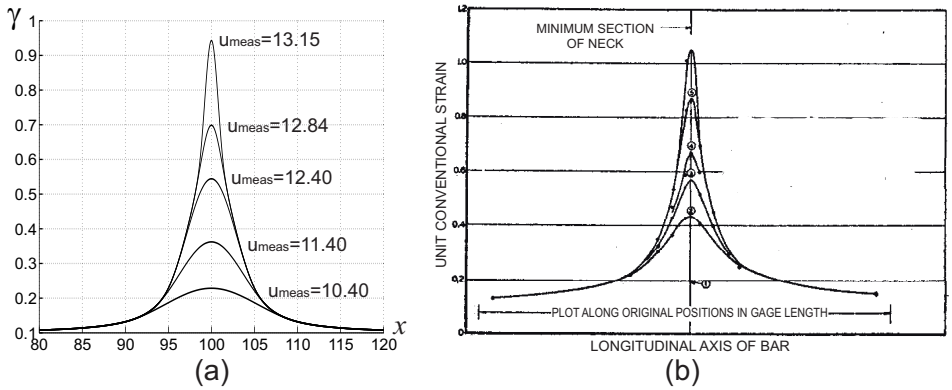

Figure 4. Diagrams of γ for different values of β: numerical (a), and experimental (b)

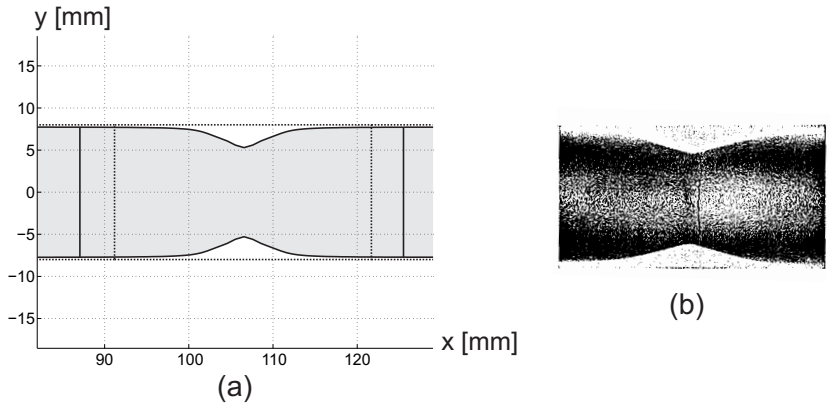

Figure 5. Necking just before ultimate failure: numerical (a), and experimental (b)

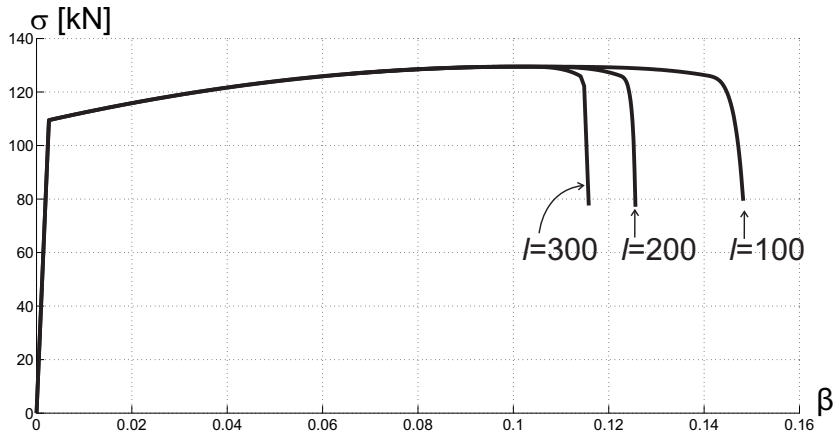

Figure 6. Force-elongation response curves for different l

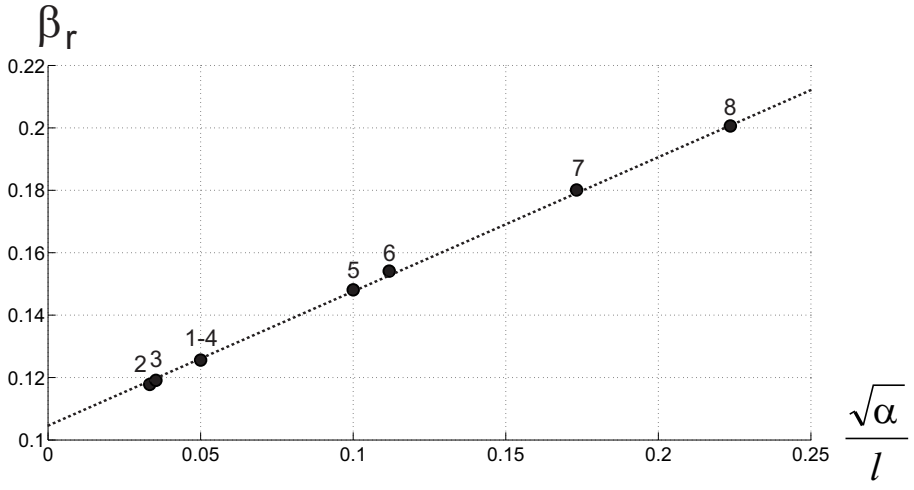

Figure 7. Numerical simulations. Dependence of the value β_r of β at rupture on the ratio $\sqrt{\alpha}/l$

References

Babadjian, J.-F.: A quasistatic evolution model for the interaction between fracture and damage, *Arch. Rational Mech. Anal.*, 200, (2011), 945-1002.

Barenblatt, G.I.: The mathematical theory of equilibrium cracks in brittle fracture, *Adv. Appl. Mech.*, 7, (1962) 55-129.

Cahn, J.W., Hilliard, J.E.: Free energy of a nonuniform system. I. Interfacial free energy, *J. Chem. Physics*, 28, (1958), 258-267.

Dal Maso, G., Toader, R.: Quasi-static crack growth in elasto-plastic materials: the two-dimensional case, *Arch. Rational Mech. Anal.*, 196, (2010), 867-906.

Del Piero, G., Lancioni, G., March, R.: A diffuse cohesive energy approach to fracture and plasticity: the one-dimensional case, Submitted, (2012).

Del Piero, G., Truskinovsky, L.: Elastic bars with cohesive energy, *Cont. Mech. Thermodynamics*, 21, (2009), 141-171.

Dugdale, D.S.: Yielding of steel sheets containing slits, *J. Mech. Phys. Solids*, 8, (1960), 100-104

Francfort, G.A., Marigo, J.-J.: Revisiting brittle fracture as an energy minimization problem, *J. Mech. Phys. Solids*, 46, (1998), 1319-1342.

Gill, P.E., Murray, W., Wright, M.H.: *Practical oprimization*, Academic Press, (1981).

Griffith, A.A.: The phenomena of rupture and flow in solids, *Phil. Trans. Roy. Soc.*, A221, (1920), 163-198.

Gurtin, M.E., Anand, L.: A theory of strain-gradient plasticity for isotropic, plastically irrotational materials. Part I: Small deformations, *J. Mech. Phys. Solids*, 53, (2005), 1624-1649.

Irwin, G.R.: Analysis of stresses and strains near the end of a crack traversing a plate, *J. Appl. Mech.*, 24, (1957), 361-364

Mielke, A.: Differential, energetic, and metric formulations for rate-independent processes, in: L. Ambrosio, G. Savare eds, *Nonlinear PDEs and Applications*, Springer Lecture Notes in Mathematics, 2028, (2011), 87-169.

Miklowitz, J.: The Influence of the Dimensional Factors on the Mode of Yielding and Fracture in Medium-Carbon Steel-II. The Size of the Round Tensile Bar, *Proc. J. Appl. Mech*, 17, (1950), 159-168.

Pham, K., Amor, H., Marigo, J.-J., Maurini, C.: Gradient damage models and their use to approximate brittle fracture, *Int. J. Damage Mechanics*, 20, (2010), 618-652.

Polak, E.: *Computational methods in optimization*, Academic Press, (1971).

J.D. Van der Waals, *On the continuity of the gas and liquid state* (in Dutch). Ph. D. Thesis, Sijthoff, Leiden, (1873).

Addresses:
Gianpietro Del Piero, Dipartimento di Ingegneria, Università di Ferrara, via Saragat 1, 44100, Ferrara, Italy, email: `dlpgpt@unife.it`,
Giovanni Lancioni, Dipartimento di Ingegneria Civile, Edile e Architettura, Università
Politecnica delle Marche, Via Brecce Bianche 1, 60131 Ancona, Italy, email: `g.lancioni@univpm.it`,
Riccardo March, Istituto per le Applicazioni del Calcolo, CNR, Via dei Taurini 19, 00185 Roma, Italy, email: `r.march@iac.cnr.it`.